Assessment of Cell Toxicity and Oxidation Catalytic Activity of Nanosized Zinc-doped Ceria UV Filter

S. Kurajica,[a] K. Mužina,[a,*] S. Keser,[b] G. Dražić,[c] and I. K. Munda[a]

[a]University of Zagreb, Faculty of Chemical Engineering and Technology, Marulićev trg 19, HR 10000 Zagreb, Croatia

[b]University of Zagreb, Faculty of Pharmacy and Biochemistry, A. Kovačića 1, HR 10000 Zagreb, Croatia

[c]National Institute of Chemistry, Hajdrihova 19, SI-1001, Ljubljana, Slovenia

doi: https://doi.org/10.15255/CABEQ.2020.1905

Original scientific paper
Received: December 15, 2020
Accepted: March 8, 2021

The abundance of cerium in natural resources, its ability to absorb UV light while being transparent to visible light, as well as low photocatalytic activity make ceria (CeO_2) a promising candidate for UV filter material in sunscreens. Doping with different elements can further decrease ceria catalytic and photocatalytic activity, thus preventing the degradation of other sunscreen ingredients. In this work, pure and zinc-doped ceria nanoparticles were prepared by a simple and environmentally benign hydrothermal synthesis, and characterized using various techniques. Fine ceria and doped ceria nanoparticles with particle sizes of 6.1±0.9 and 4.2±0.4 nm were prepared. In both samples, cubic ceria was the only crystalline phase, but the homogeneous distribution of zinc in the doped sample was confirmed by energy dispersive X-ray spectrometry. Nanoparticles exhibited transparency in the visible region and absorbance in the UV region with band gap of 3.23 to 3.14 eV for pure and doped sample, respectively. The oxidation stability time, determined through Castor oil oxidation process, was 23 hours for the pure and 15 hours for the doped sample, which is quite satisfactory. *In vitro* cytotoxicity study showed that the prepared nanoparticles were well tolerated by human skin keratinocytes (HaCaT cell line) with no significant differences in skin cells viability. However, further investigations on *in vivo* systems are necessary to reach a firm conclusion regarding the toxicity of ceria and doped ceria nanoparticles, and other potential dopants should be considered for improvement of ceria properties for sunscreen application.

Keywords:
doped ceria, hydrothermal synthesis, HaCaT cell line, cytotoxicity

Introduction

Beside applicability in various environmental and energy-related applications,[1] ceria (CeO_2) nanoparticles also have a potential application as sunscreen ingredient since they absorb UV radiation, while being relatively transparent to visible light.[2] The use of UV absorbing metallic oxides in sunscreen in the form of nanoparticles makes sunscreen layer on the skin invisible since their particle size is far below the wavelength of visible light and thus scattering is avoided.[3] TiO_2 and ZnO, which are commonly used as inorganic UV blocking filters in sunscreens, show pronounced photocatalytic activity facilitating the generation of reactive oxygen species that oxidize and degrade the ingredients of sunscreen formulations.[4] Also, due to photocatalytic generation of reactive oxygen species, TiO_2 and ZnO could damage the skin cells.[5] In comparison to TiO_2 and ZnO, ceria has lower photocatalytic activity, although it is still capable of catalyzing the oxidation of organic compounds.[4] On the other hand, it appears that ceria nanoparticles have radical scavenging capabilities as well as the potential to mitigate oxidative stress that triggers different pathological conditions.[6] However, cytotoxicity assessment studies of ceria nanoparticles are contradictory[7] and, so far, ceria is rarely used in commercial sunscreen formulations.

The properties of nanoparticles can be tuned by doping the host crystal structure with various elements.[8] The ceria catalytic activity relies on oxygen release ability, and it was established that oxygen release can be reduced by doping with a metal ion having lower valence in comparison to Ce^{4+}.[2,9] Zn^{2+} meets this criterion, and there is a limited number of papers on zinc-doped ceria: Li *et al.*[10] prepared ZnO-doped CeO_2 particles via soft solution route having particle sizes between 3 and 7 nm. They noted that the solubility limit of ZnO in CeO_2 is greater

*Corresponding author: Katarina Mužina, E-mail: kmuzina@fkit.hr

than 50 %. Doped ceria retained UV radiation opacity and visible light transparency similar to non-doped ceria, while the photocatalytic activity of zinc-doped ceria had substantially decreased. Chai and Wang[11] prepared fine particles of zinc and cerium oxide powder via combustion synthesis route. They showed that photocatalytic activity and oxidation catalytic activity of prepared sample had decreased in comparison to pure CeO_2, while its ultraviolet absorption in the UV range was excellent. Fonseca de Lima *et al.*[4] prepared a mixture of CeO_2 and ZnO in 1:9 molar ratio via non-alkoxide sol-gel process. They report average particle sizes of prepared powders between 50 and 100 nm, higher UV absorption, and lower photocatalytic activity for the oxidation of organic material in comparison to pure oxides. Wu *et al.*[9] prepared ZnO-doped CeO_2 by mechanochemical synthesis yielding with 75–100 nm particles. They showed that catalytic ability for oil oxidation process decreased with the increase in the amount of zinc. Kellici *et al.*[12] prepared a series of ZnO-doped CeO_2 samples by continuous hydrothermal flow synthesis technique. They concluded that the solubility limit of ZnO in CeO_2 was about 20 %. Pure ceria had particle size of approximately 3.7 nm, while particle sizes of doped samples were not reported. Doped samples had steeper UV-Vis absorption edge and blueshifted band gap. Govindarajan and Nithya[13] prepared cerium thin films doped with 4 and 8 % of Zn by spray pyrolysis technique. They noted a small redshift of the band gap, and decrease in transmittance in the visible part of spectrum.

The synthetic route greatly affects the size and shape of nanoparticles and consequently their properties.[12] Various methods of ceria and doped ceria preparation are described in the literature, such as precipitation, mechanochemical synthesis, sol-gel process, hydrothermal synthesis, etc.[14] The advantages of hydrothermal method are simplicity, affordability, and environmental benignity.[15] Recently, we presented an optimized hydrothermal synthesis of ceria yielding with fine nanoparticles.[16] We also reported on the ability of various transition metals, zinc among them, to enter the ceria crystal lattice.[17]

Nanoparticles exposure is recognized as a possible source of damage to human beings and the environment. Therefore, reliable tests on the evaluation of threats are required, and *in vitro* cell toxicity assays are of utmost importance for nanoparticles health risk assessment.[18] While ceria cytotoxicity is well investigated, we were unable to find a paper on zinc-doped ceria cytotoxicity. Cell lines should be selected on the basis of possible modes of contacts and uptakes in humans or possible metabolic targets.[18] Therefore, if nanoparticles aimed for sunscreen ingredient are to be investigated, it would be practical to select a skin cell line for cytotoxicity assay. Surprisingly, even when pure ceria is considered, cell lines in cytotoxicity assays are targeted on various cell lines, but rarely on skin cells. There is only one study where cerium oxide nanopowders cytotoxicity for NCTC2544 keratinocytes cell line was compared to commercially available sunscreens containing zinc oxide.[19] No impact of cerium oxide particles on cell growth was established, while a reduction in cell viability was noted after cell treatment with diluted sunscreen containing all the sunscreen ingredients. Studies on other cell lines include cerium oxide nanoparticles cytotoxicity testing on human prostate cancer cell line (PC-3), and normal mouse fibroblast cell line (L929),[20] where nanoparticles were found to be cytotoxic towards PC-3, but nontoxic towards L929 cell lines. Another study tested cerium oxide nanoparticles on cultured human lung-cancer cells (A549), where cell viability decreased as a function of nanoparticle dose and exposure time.[21] Cytotoxicity of cerium oxide nanoparticles and microparticles was compared on human neuroblastoma cell line (IMR32) and a dose-dependent effect was found for higher concentrations of nanoparticles, whereas microparticles induced no significant changes in cell viability.[22] The effects of short-term (24 h) and long-term (10 days) exposure of three different cell lines: human alveolar adenocarcinoma cell line (A549), human colorectal adenocarcinoma cell line (CaCo2), and human hepatic carcinoma cell line (HepG2) to ceria nanoparticles was tested over a wide range of nanoparticle concentrations. Cytotoxicity study showed almost no short-term exposure toxicity to ceria nanoparticles on any of the tested cell lines, but long-term exposure proved toxic for all tested cell lines.[18]

Therefore, in this study, the skin cell line was used for the comparison of cytotoxicity of ceria and doped ceria nanoparticles for the first time. *In vitro* nanoparticles cytotoxicity was tested on HaCaT human keratinocytes cell line over a concentration range between 50 μg mL^{-1} to 150 μg mL^{-1}. Other key properties for utilization of hydrothermally derived nanoparticles as a sunscreen component were also evaluated.

Materials and methods

Pure ceria synthesis procedure has been described elsewhere.[23] Briefly, 0.8 mmol of $Ce(SO_4)_2 \cdot 4H_2O$ was dissolved in 80 cm^3 of NaOH solution (c = 8 mol dm^{-3}). The solution was placed in a 100-cm^3 capacity Teflon-lined stainless-steel autoclave, tightly sealed and kept in a temperature-controlled oven for 16 h at 120 °C. The ob-

tained product was centrifuged at 3500 rpm, and the precipitate was washed with demineralized water with the help of sonification. Procedure was repeated three times, and the precipitate was dried at 60 °C for 24 h in static air. Zinc-doped sample was prepared in the same manner, but with 0.72 mmol of $Ce(SO_4)_2 \cdot 4H_2O$, and 0.08 mmol of $ZnSO_4 \cdot 7H_2O$.

The morphologies of the samples were investigated using transmission electron microscopy (TEM) on Jeol ARM 200 CF microscope with accelerating voltage of 80 kV coupled with Jeol Centurio 100 for energy dispersive X-ray spectrometry (EDS). For the image analysis, ImageJ program[24] was used.

X-ray diffraction (XRD) analysis was performed on Shimadzu XRD 6000 diffractometer with CuKα radiation operating at 40 kV and 30 mA with the aim of identifying the crystal phases in the samples. Data were collected in a step scan mode between 20 and 100 °2θ with steps of 0.02 °2θ and counting time of 0.6 s. The crystallite sizes were determined through the Scherrer's equation: $D = k\lambda/\beta\cos\theta$, where D is the crystallite size in nm, k is the shape factor which is 0.94 for spherical crystallites with cubic symmetry, λ is the CuKα radiation wavelength which equals 0.15405 nm, β is the peak full width at half maximum corrected for instrumental broadening, and θ is the Bragg angle.[25]

The UV–Vis reflectance spectra were acquired using diffuse reflectance spectrometer (DRS) Shimadzu UV–3101PC equipped with an integrating sphere. Barite ($BaSO_4$) was used as a white reference, and samples were diluted with $BaSO_4$ in a ratio of 1:4. Obtained spectra were transformed using Kubelka-Munk transformation: $F(R)=(1-R)^2/(2R)$, where $F(R)$ is proportional to the extinction coefficient (α), and R is the reflectance. Band gaps, E_g, were determined by plotting $(F(R)hv)^n$ vs. photon energy (hv), the so-called Tauc's plot, where h is the Planck's constant, v is frequency, the quotient of light velocity and wavelength (λ/m), while n is the coefficient associated with electronic transition, and for direct allowed transitions equals 2. Band gap was obtained by linear fitting of the $(F(R)hv)^2$ vs. hv curve and line extrapolation onto the energy axis.

The photocatalytic activity for the organic material oxidation was determined by the accelerated oxidation Rancimat method (Metrohm 873 Biodiesel Rancimat)[26] using Castor oil as the model oxidizing material. In the Rancimat method, the oil aging process is accelerated by exposing it to heat and air flow. The time required for oxidation to take place at a high rate is called oxidation stability index or induction time. For the analysis, 1 g of the powder samples were mixed with 10.0 mL of Castor oil, and homogenized using an ultrasonic bath for 30 min. The samples were maintained for 24 h at 120 °C under air bubbling with the flow rate of 10 L h^{-1}. Catalytic activity was determined by trapping volatile molecules formed by the oxidation of Castor oil in 100 mL of deionized water and measuring the increase in the electric conductivity. The initial water conductivity was subtracted from the measured conductivities, and the results shown as the dependence of conductivity on time.

Cytotoxicity of nanocrystalline ceria and doped ceria was studied using HaCaT cell lines. Human keratinocyte cell line HaCaT (Cell Line Services, Germany) were cultured in Dulbecco's Modified Eagle's Medium (DMEM; Gibco, Invitrogen, Paisley, UK) supplemented with 10 % fetal bovine serum (Gibco, Thermo Fisher Scientific, USA) and a mixture of penicillin, streptomycin and amphotericin B (Lonza, Basel Switzerland). For the assessment of potential cytotoxicity of the three types of nanoparticles, HaCaT cells were seeded onto 96-well plates at a density of 10^4 cells/well, and left for 48 hours to reach confluence. Stock solutions (0.5 mg mL^{-1}) of pure, zinc-doped ceria and titanium dioxide nanoparticles were prepared in non-supplemented cell culture medium in order to avoid aggregates of nanoparticles and proteins from fetal bovine serum. They were sonicated before use and diluted to concentrations of 50, 100, and 150 μg mL^{-1} also with non-supplemented cell culture medium. Prior to treatment with nanoparticles, cell culture medium was removed, and cells washed with PBS. Cells were then exposed for 24 hours to different nanoparticle concentrations. Cells incubated in non-supplemented culture medium were used as a negative control. The testing was carried out in hexaplicates. After the treatment, the cells were washed twice with PBS and complete medium was added. *In vitro* cytotoxicity was determined after 24 hours by the MTT assay. An amount of 20 μL of MTT (3-(4,5-dimethylthiazol-2-yl)-2,5-diphenyltetrazolium bromide; Sigma-Aldrich, St. Louis, USA) solution in DMEM (5 μg mL^{-1}) was added to each well, and the cells were then incubated for 1 hour at 37 °C. After incubation, the medium was removed, and 100 μL of isopropanol was added to each well. The amount of formazan was quantified spectrophotometrically at 570 nm (Victor, Perkin-Elmer, USA). Mitochondrial activity is expressed relative to that in the control group treated with non-supplemented cell culture medium. Statistical data analyses of the three groups were performed using two-way ANOVA and Tukey's multiple comparison tests, and the means were considered significantly different when $p < 0.05$. Calculations were performed with the GraphPad 8 Prism program (GraphPad Software, Inc., San Diego, USA).

Citotoxicity measurements were also conducted on commercial TiO_2 nanoparticles (Evonik P25)

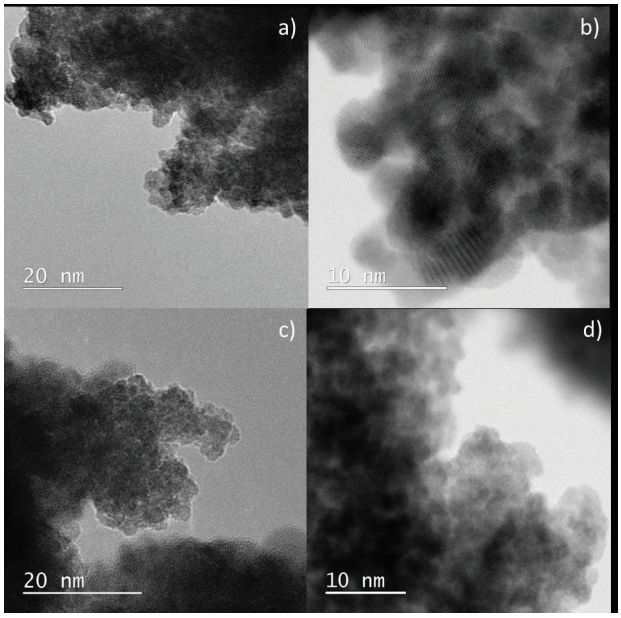

Fig. 1 – *STEM-BF micrographs of the pure (a and b), and doped (c and d) samples*

for comparison, since, due to its low photoallergic potential and high photostability, TiO_2 is the most common inorganic UV filter in commercial sunscreen formulations.[27–30]

Results and discussion

In order to obtain insight into morphology, particle size, and composition of ceria and doped ceria, samples were analyzed using HRTEM and EDS. Representative HRTEM micrographs are given in Fig. 1. Both samples display fine agglomerates of roughly spherical nanoparticles, and no notable difference in morphology between the pure and the doped sample was observed. The obtained shape was probably due to the lack of energy necessary for a particle to reach equilibrium, which is a consequence of low temperature used during the synthesis.[31] The average particle sizes, calculated from HRTEM images using ImageJ software package, were 6.1±0.9 nm and 4.2±0.4 nm for pure and doped ceria, respectively. The reduction in particle size with the introduction of dopant could be explained by the decrease of ceria concentration in the system, causing the retardation of diffusion rate and hindering the growth.[32] Lattice fringes distances in both samples were 0.31±0.01 nm, which is the typical distance for (111) planes of ceria fluorite structure with the lowest surface energy.[33]

The presence and distribution of elements in the samples was tested through EDS analysis, (Fig. 2). TEM-EDS mapping revealed a homogeneous distribution of cerium and oxygen in both samples suggesting that ceria was the only phase present. Additionally, the distribution of zinc in the zinc-doped sample also appeared homogeneous proving its entrance in the ceria crystal lattice.

Phase composition and purity of the prepared samples were examined by XRD. XRD patterns of the pure and doped samples are presented in Fig. 3. Both patterns are characterized by the presence of ceria diffraction peaks (ICDD PDF No. 34-0394), and no additional peaks were noted for the doped

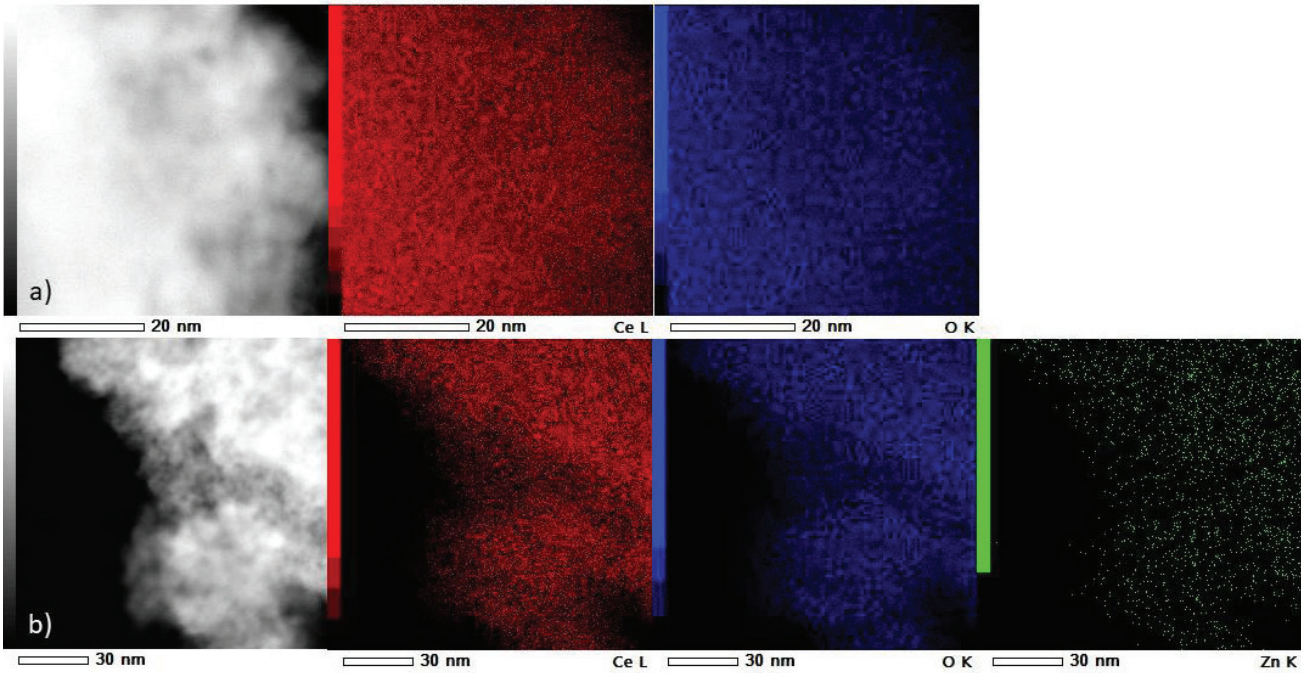

Fig. 2 – *STEM-ADF image and EDS mapping of the pure (a) and doped (b) samples*

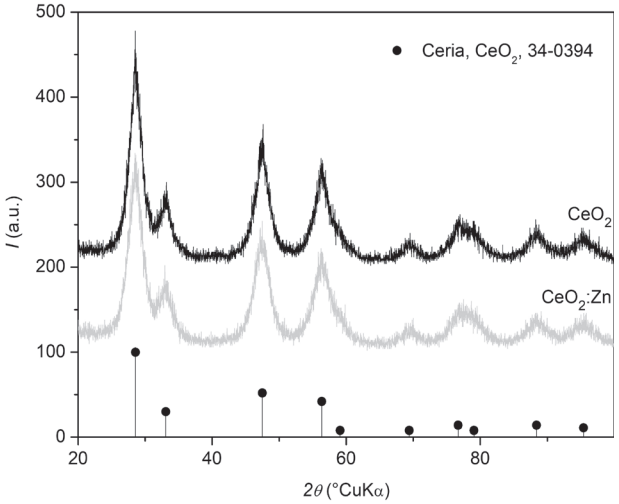

Fig. 3 – *Diffraction patterns of the pure and doped samples*

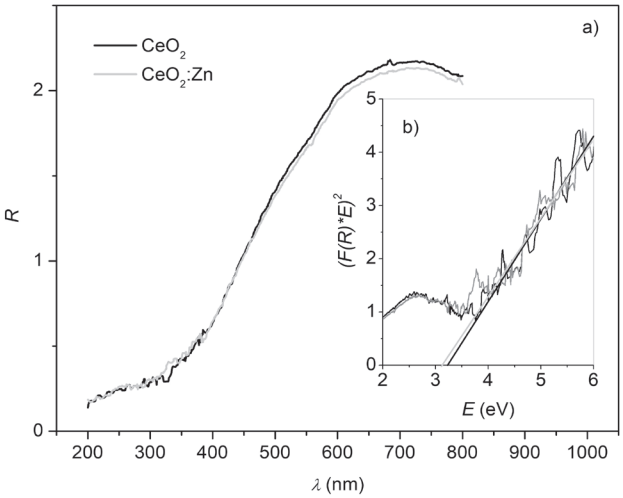

Fig. 4 – *UV-Vis diffuse reflectance spectra (a) and Tauc's plots (b) of the pure and doped samples*

sample, suggesting that no other phases were present in the amount detectable by XRD. Broad peaks indicate that crystallites are in the nanometers range. Unfortunately, the broadness of the XRD peaks made the observation of any peak shift due to the entrance of zinc in the crystal structure of ceria impossible. No significant differences in peak position, broadness, and intensity for the pure and doped samples were noted. The crystallite sizes determined using the Scherrer's equation were 4.5±0.1 nm and 4.0±0.1 nm for pure and Zn-doped ceria, respectively. It can be observed that there is a concordance of calculated crystallite sizes and particle sizes determined from TEM micrographs, which means that a particle is equivalent to a crystallite.

The XRD, TEM, and EDS analyses clearly show that the hydrothermal synthesis enabled the preparation of very small, high-purity crystallites. For the doped sample, it may be stated that Zn had incorporated into the ceria crystal lattice since no other phases than ceria appeared on the XRD pattern, but the EDS analysis clearly showed a homogeneous distribution of Zn throughout the sample. Further analyses were aimed at examining properties important for the application of ceria in sunscreen – band gap value, catalytic activity, and cytotoxicity.

UV-Vis reflectance spectra and Tauc's plots of the prepared samples are presented in Fig. 4. It appears that the reflectance in the entire measured area is almost the same for both samples. In the reflectance spectra, low reflectance indicates high absorption and vice versa. Therefore, both prepared samples show high absorption in the UV region and transparency in the visible region. Small difference could be observed in the reflectance curve slope. From the Tauc's plot, the band gap of 3.23 eV was obtained for the pure sample, which is very close to the literature value (3.19 eV).[34] The doped sample band gap is redshifted and yields 3.14 eV. Govindarajan *et al.*[13] and Nurhasanah *et al.*[35] both report on the reduction in the band gap value with the increase in Zn doping in the CeO_2 samples. The decrease in the band gap could be attributed to lattice defects and strain.[36] Namely, when Zn, having lower valence and smaller radius, is incorporated into the ceria crystal lattice, the number of oxygen defects increases due to the maintenance of the lattice electroneutrality and the increased reduction in Ce^{4+} to Ce^{3+}.[35]

The results of oxidation catalytic activity via Rancimat test for Castor oil are shown in Fig. 5. As can be observed, both samples (ceria and zinc-doped ceria) show similar tendencies during the first 15 h of the experiment. However, after 15 h, the conductivity of water-dissolving degradation products of Castor oil mixed with zinc-doped ceria begin to grow exponentially, and therefore 15 h could be declared as the oxidation stability index or induction time of the zinc-doped ceria. By the same criterion, the oxidation stability time of pure ceria was found to be 23 h. This result comes as a surprise since the literature reports greater oil oxidation stability in the presence of zinc-doped ceria in comparison with pure ceria, i.e., the decrease in ceria oxidation catalytic activity by doping with zinc.[9,10,37] We believe that greater catalytic activity of the zinc-doped sample is a consequence of smaller particle size, i.e., greater specific surface area, which is one of the most beneficial properties for catalytic application.[16] However, taking into consideration the accelerated oxidation conditions (high temperature and rapid air flow), the oxidation stability of Castor oil in the presence of both nanoparticles, ceria, and doped ceria, can be rated as satisfactory.

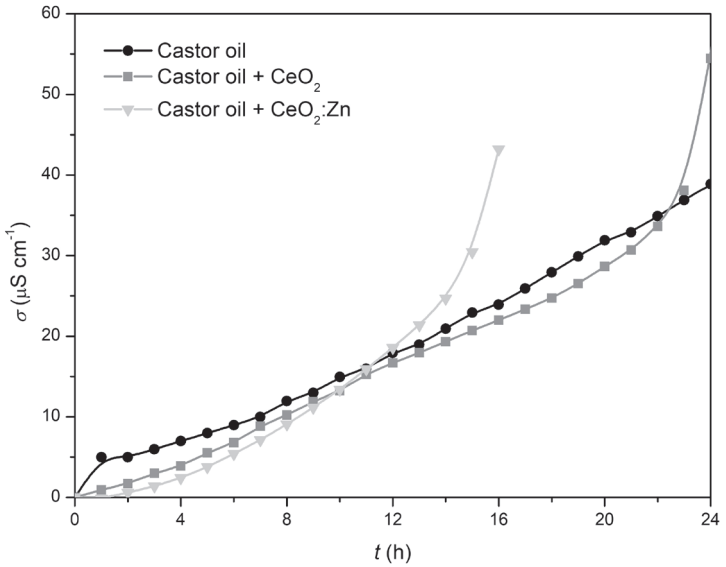

Fig. 5 – *Rancimat test results for pure Castor oil, Castor oil with ceria, and Castor oil with zinc-doped ceria*

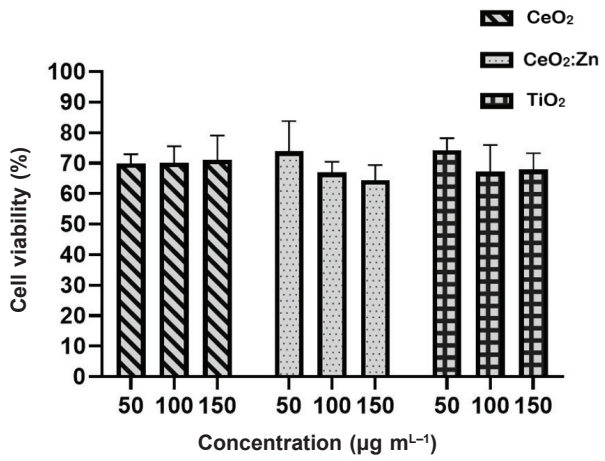

Fig. 6 – *HaCaT cells viability (%) after 24 h of incubation at 37 °C treated with ceria, zinc-doped ceria, and titania nanoparticles as determined by the MTT assay. The values denote the mean ± S.D. (n = 6).*

As stated in the introduction, there has been a variety of studies on cytotoxicity effects of ceria nanoparticles on different cell lines, but the selected lines mostly do not match the sunscreen route of application. Since our intention was to study these nanoparticles as potential ingredients for use in sunscreen preparations, HaCaT human keratinocyte cell line was chosen. To the best of our knowledge, this is the first cytotoxicity assay of ceria and zinc-doped ceria nanoparticles carried out on this cell line.

After a preliminary MTT assay in a broad range of concentrations was performed, 50, 100, and 150 μg mL^{-1} were selected as concentrations for further testing, in order to ensure that the biocompatibility study covered a wide enough range of concentrations for all three types of nanoparticles, and also to be able to compare the concentrations with other published results regarding toxicity studies.[19,28,38,39]

HaCaT cells viability after treatment with ceria, zinc-doped ceria, and titania nanoparticles after 24 h of incubation at 37 °C are shown in Fig. 6. According to the guideline for determination of *in vitro* cytotoxicity of medical devices, materials are considered nontoxic if the viability of cells is ≥ 70 % after exposure.[40] The results of the biocompatibility study (Fig. 6) indicated that all three types of nanoparticles were well tolerated by the keratinocytes. Only in cases of 100 and 150 μg mL^{-1} of ceria doped with Zn and titanium dioxide nanoparticles, cell viability marginally decreased below 70 %, but still not enough to show any statistical significance compared to doses of 50 μg mL^{-1} ($p > 0.05$). There was no significant difference between nanoparticle types, and therefore it can be concluded that ceria and ceria doped with zinc nanoparticles are as safe as titanium dioxide nanoparticles in these conditions.

Due to great differences in experimental conditions, no direct comparison to any other study can be made. Cerium oxide nanoparticles were also found nontoxic to NCTC2544 keratinocytes cell line[19] and to normal mouse fibroblast cell line (L929).[20] On the other hand, cerium oxide nanoparticles were proven cytotoxic for human prostate cancer cell line (PC-3),[20] human lung cancer cells (A549),[21] and human neuroblastoma cell line (IMR32).[20] However, it was noted that cell viability was a function of nanoparticle dose and exposure time,[21,22] e.g., almost no short-term exposure toxicity to ceria nanoparticles on human alveolar adenocarcinoma cell line (A549), human colorectal adenocarcinoma cell line (CaCo2), and human hepatic carcinoma cell line (HepG2) was noted, while long-term exposure proved toxic for all tested cell lines.[18] There is also a lack of comparison of cerium oxide particles influence on the cell viability with any pure inorganic UV filter. Therefore, further investigations are necessary, particularly on *in vivo* systems, in order to attain a firm conclusion regarding the toxicity of ceria and ceria doped with zinc nanoparticles.

Conclusions

Pure ceria and zinc-doped ceria samples were prepared by hydrothermal synthesis. Very small, roughly spherical particles were obtained. While the particle size of the pure sample was 6.1±0.9 nm, the particle size of the doped sample was reduced to 4.2±0.4 nm. The crystallite sizes calculated from the Scherrer equation are in concordance with the obtained particle sizes. According to XRD analysis,

cubic ceria was the only crystal phase present in both samples, but the presence of zinc and its homogeneous distribution in the doped sample were verified by EDS mapping, indicating that Zn had incorporated into the ceria crystal lattice. No significant differences were noted in the UV absorption and visible region transparency between the pure and the doped ceria, but a small redshift of the band gap from 3.23 to 3.14 eV was observed for the doped sample. Castor oil oxidation stability in the presence of ceria and zinc-doped ceria was found satisfactory. HaCaT human keratinocytes cells showed good viability in a wide range of ceria and zinc-doped ceria concentrations. No significant differences in cell viability between investigated nanoparticles, as well as titania nanoparticles were noted. Present study shows that nanosized ceria and zinc-doped ceria are both promising materials for utilization as UV-filters in sunscreen. Further investigations will focus on doping of ceria with different elements, which could have a stronger influence on improving the properties of ceria, as well as *in vivo* cytotoxicity studies, which are necessary for the practical application of this material in sunscreen.

ACKNOWLEDGEMENT

This work has been fully supported by Croatian Science Foundation under the project IP-01-2018-2963. The sustenance of the University of Zagreb is gratefully acknowledged. L. Konjević i M. Tirić Unetić from INA d.d. Central Testing Laboratory are much obliged for conducting the Rancimat test.

References

1. *Montini, T., Melchionna, M., Monai, M., Fornasiero, P.,* Fundamentals and catalytic applications of CeO_2-based materials, Chem. Rev. **116** (2016) 5987. doi: https://doi.org/10.1021/acs.chemrev.5b00603
2. *Yabe, S., Sato, T.,* Cerium oxide for sunscreen cosmetics, J. Solid State Chem. **171** (2003) 7. doi: https://doi.org/10.1016/S0022-4596(02)00139-1
3. *Faure, B., Salazar-Alvarez, G., Ahniyaz, A., Villaluenga, I., Berriozabal, G., De Miguel, Y. R., Bergström, L.,* Dispersion and surface functionalization of oxide nanoparticles for transparent photocatalytic and UV-protecting coatings and sunscreens, Sci. Technol. Adv. Mater. **14** (2013) (023001) 1. doi: https://doi.org/10.1088/1468-6996/14/2/023001
4. *Fonseca de Lima, J., Figueredo Martins, R., Neri, C. R., Serra, O. A.,* ZnO:CeO_2-based nanopowders with low catalytic activity as UV absorbers, Appl. Surf. Sci. **255** (2009) 9006. doi: https://doi.org/10.1016/j.apsusc.2009.06.071
5. *Hidaka, H., Kobayashi, H., Koike, T., Sato, T., Serpone, N.*, DNA damage photoinduced by cosmetic pigments and sunscreen agents under solar exposure and artificial UV illumination, J. Oleo Sci. **55 (5)** (2006) 249. doi: https://doi.org/10.5650/jos.55.249
6. *Xia, T., Kovochich, M., Liong, M., Madler, L., Gilbert, B., Shi, H., Yeh, J. I., Zink, J. I., Nel, A. E.,* Comparison of the mechanism of toxicity of zinc oxide and cerium oxide nanoparticles based on dissolution and oxidative stress properties, ACS Nano **2** (2008) 2121. doi: https://doi.org/10.1021/nn800511k
7. *Forest, V., Leclerc, L., Hochepied, J. F., Trouvé, A., Sarry, G., Pourchez, J.*, Impact of cerium oxide nanoparticles shape on their in vitro cellular toxicity, Toxicol. in Vitro **38** (2017) 136. doi: https://doi.org/10.1016/j.tiv.2016.09.022
8. *Mogensen, M., Sammes, N. M., Tompsett, G. A.*, Physical, chemical and electrochemical properties of pure and doped ceria, Solid State Ion. **129** (2000) 63. doi: https://doi.org/10.1016/S0167-2738(99)00318-5
9. *Wu, W., Li, S., Liao, S., Xiang, F., Wu, X.,* Preparation of new sunscreen materials $Ce_{1-x}Zn_xO_{2-x}$ via solid-state reaction at room temperature and study on their properties, Rare Metals **29 (2)** (2010) 149. doi: https://doi.org/10.1007/s12598-010-0026-2
10. *Li, R., Yabe, S., Yamashita, M., Momose, S., Yoshida, S., Yin, S., Sato, T.,* UV-shielding properties of zinc oxide-doped ceria fine powders derived via soft solution chemical routes, Mater. Chem. Phys. **75** (2002) 39. doi: https://doi.org/10.1016/S0254-0584(02)00027-5
11. *Chai, X., Wang, D.,* UV-shielding and catalytic characteristics of nanoscale zinc-cerium oxides, Journal of Wuhan University of Technology-Mater. Sci. Ed. **22** (2007) 622. doi: https://doi.org/10.1007/s11595-006-4622-9
12. *Kellici, S., Gong, K., Lin, T., Brown, S., Clark, R. J. H., Vickers, M., Cockcroft, J. K., Middelkoop, V., Barnes, P., Perkins, J. M., Tighe, C. J., Darr, J. A.,* High-throughput continuous hydrothermal flow synthesis of Zn–Ce oxides: Unprecedented solubility of Zn in the nanoparticle fluorite lattice, Phil. Trans. R. Soc. A **368** (2010) 4331. doi: https://doi.org/10.1098/rsta.2010.0135
13. *Govindarajan, D., Nithya, C. K.,* Zinc doped cerium oxide thin films prepared by spray pyrolysis method, Int. J. Curr. Res. **7** (2015) 13922.
14. *Dahl, A., Self, W.,* Cerium oxide nanoparticles: A brief review on their synthesis methods and biomedical applications, Antioxidants **7** (2018) 97. doi: https://doi.org/10.3390/antiox7080097
15. *Sun, C., Li, H., Chen, L.,* Nanostructured ceria-based materials: Synthesis, properties and applications, Energy Environ. Sci. **5** (2012) 8475. doi: https://doi.org/10.1039/C2EE22310D
16. *Kurajica, S., Minga, I., Guliš, M., Mandić, V., Simčić, I.,* High surface area ceria nanoparticles via hydrothermal synthesis experimental design, J. Nanomater. **2016** (7274949) (2016) 1. doi: https://doi.org/10.1155/2016/7274949
17. *Kurajica, S., Mužina, K., Dražić, G., Matijašić, G., Duplančić, M., Mandić, V., Župančić, M., Munda, I. K.,* A comparative study of hydrothermally derived Mn, Fe, Co, Ni, Cu and Zn doped ceria nanocatalysts, Mat. Chem. Phys. **244** (122689) (2020) 1. doi: https://doi.org/10.1016/j.matchemphys.2020.122689
18. *De Marzi, L., Monaco, A., De Lapuente, J., Ramos, D., Borras, M., Di Gioacchino, M., Santucci, S., Poma, A.,* Cytotoxicity and genotoxicity of ceria nanoparticles on different cell lines *in vitro*, Int. J. Mol. Sci. **14** (2013) 3065. doi: https://doi.org/10.3390/ijms14023065
19. *Boutard, T., Rousseau, B., Couteau, C., Tomasoni, C., Simonnard, C., Jacquot, C., Coiffard, L. J. M., Konstantinov, K., Devers, T., Roussakis*, C., Comparison of photoprotec-

tion efficiency and antiproliferative activity of ZnO commercial sunscreens and CeO_2, Mater. Lett. **108** (2013) 13. doi: https://doi.org/10.1016/j.matlet.2013.06.085

20. *Renu, G., Divya, Rani, V. V., Nair, S. V., Subramanian, K. V. R., Lakshmanan, V. K.,* Development of cerium oxide nanoparticles and its cytotoxicity in prostate cancer cells, Adv. Sci. Lett. **5** (2012) 1. doi: https://doi.org/10.1166/asl.2012.3312
21. *Lin, W., Huang, Y., Zhou, X., Ma, Y.*, Toxicity of cerium oxide nanoparticles in human lung cancer cells, Int. J. Toxicol. **25** (2006) 451. doi: https://doi.org/10.1080/10915810600959543
22. *Kumari, M., Singh, S. P., Chinde, S., Rahman, M. F., Mahboob, M., Grover, P.,* Toxicity study of cerium oxide nanoparticles in human neuroblastoma cells, Int. J. Toxicol. **33 (2)** (2014) 86. doi: https://doi.org/10.1177/1091581814522305
23. *Duplančić, M., Kurajica, S., Tomašić, V., Minga, I.,* Catalytic oxidation of toluene on hydrothermally prepared ceria nanocrystals, Chem. Biochem. Eng. Q. **31** (2017) 375. doi: https://doi.org/10.15255/CABEQ.2017.1098
24. *Schneider, C. A., Rasband, W. S., Eliceiri, K. W.,* NIH Image to ImageJ: 25 years of image analysis, Nat. Methods **9** (2012) 671. doi: https://doi.org/10.1038/nmeth.2089
25. *Klug, H. P., Alexander, L. E.*, X-Ray diffraction procedures for polycrystalline and amorphous materials, 2nd ed., John Wiley & Sons Inc., New York, 1974, pp. 687-703. doi: https://doi.org/10.1002/bbpc.19750790622
26. Metrohm-URL: https://www.metrohm.com/en-in/products/stability-measurement/rancimat (1.7.2020.)
27. *Palm, M. D., O'Donoghue, M. D.,* Update on photoprotection, Dermatol. Ther. **20** (2007) 360. doi: https://doi.org/10.1111/j.1529-8019.2007.00150.x
28. *Crosera, M., Prodi, A., Mauro, M., Pelin, M., Florio, C., Bellomo, F., Adami, G., Apostoli, P., De Palma, G., Bovenzi, M., Campanini, M., Filon, F. L.,* Titanium dioxide nanoparticle penetration into the skin and effects on HaCaT cells, Int. J. Environ. Res. Public Health **12** (2015) 9282. doi: https://doi.org/10.3390/ijerph120809282
29. *Peters, K., Unger, R. E., Kirkpatrick, C. J., Gatti, A. M., Monari, E.,* Effects of nano-scaled particles on endothelial cell function *in vitro*: Studies on viability, proliferation and inflammation, J. Mater. Sci. Mater. Med. **15** (2004) 321. doi: https://doi.org/10.1023/B:JMSM.0000021095.36878.1b
30. *Yamamoto, A., Honma, R., Sumita, M., Hanawa, T.,* Cytotoxicity evaluation of ceramic particles of different sizes and shapes, J. Biomed. Mater. Res.: A **68** (2004) 244. doi: https://doi.org/10.1002/jbm.a.20020
31. *Hu, C., Zhang, Z., Liu, H., Gao, P., Wang, Z. L.*, Direct synthesis and structure characterization of ultrafine CeO_2 nanoparticles, Nanotechnology **17** (2006) 5983. doi: https://doi.org/10.1088/0957-4484/17/24/013
32. *Vladut, C. M., Mihaiu, S., Mocioiu, O. C., Atkinson, I., Pandele-Cusu J., Anghel E. M., Calderon-Moreno, J. M., Zaharescu, M.,* Thermal studies of Mn^{2+}-doped ZnO powders formation by sol–gel method, J. Therm. Anal. Calorim. **135** (2019) 2943. doi: https://doi.org/10.1007/s10973-018-7592-1
33. *Pan, C., Zhang, D., Shi, L.,* CTAB assisted hydrothermal synthesis, controlled conversion and CO oxidation properties of CeO_2 nanoplates, nanotubes, and nanorods, J. Solid State Chem. **181** (2008) 1298. doi: https://doi.org/10.1016/j.jssc.2008.02.011
34. *Kumar, E., Selvarajana, P., Muthuraj, D.,* Synthesis and characterization of CeO_2 nanocrystals by solvothermal route, Mater. Res. **16** (2013) 269. doi: https://doi.org/10.1590/S1516-14392013005000021
35. *Nurhasanah, I., Sutanto, H., Futikhaningtyas, R.,* Optical properties of Zn-doped CeO_2 nanoparticles as function of Zn content, Adv. Mat. Res. **896** (2014) 108. doi: https://doi.org/10.4028/www.scientific.net/AMR.896.108
36. *Tiwari, S., Rathore, G., Patra, N., Yadav, A. K., Bhattacharaya, D., Jah, N., S., Tseng, C. M., Liu, S. W., Biring, S., Sen, S.,* Oxygen and cerium defects mediated changes in structural, optical and photoluminescence properties of Ni substituted CeO_2, J. Alloy Compd. **782** (2019) 689. doi: https://doi.org/10.1016/j.jallcom.2018.12.009
37. *Yabe, S., Yamashita, M., Momose, S., Tahira, K., Yoshida, S., Li, R., Yin, S., Sato, T.,* Synthesis and UV-shielding properties of metal oxide doped ceria via soft solution chemical processes, Int. J. Inorg. Mater. **3** (2001) 1003. doi: https://doi.org/10.1016/S1466-6049(01)00198-2
38. *Jaeger, A., Weiss, D. G., Jonas, L., Kriehuber, R.,* Oxidative stress-induced cytotoxic and genotoxic effects of nano-sized titanium dioxide particles in human HaCaT keratinocytes, Toxicology **296** (2012) 27. doi: https://doi.org/10.1016/j.tox.2012.02.016
39. *Fujitaa, K., Horiea, M., Kato, H., Endohc, S., Suzuki, M., Nakamura, A., Miyauchi, A., Yamamoto, K., Kinugasac, S., Nishioa, K., Yoshidaa, Y., Iwahashi, H., Nakanishi, J.,* Effects of ultrafine TiO_2 particles on gene expression profile in human keratinocytes without illumination: Involvement of extracellular matrix and cell adhesion, Toxicol. Lett. **191** (2009) 109. doi: https://doi.org/10.1016/j.toxlet.2009.08.011
40. ISO 10993-5: Biological evaluation of medical devices – Part 5: Tests for in vitro cytotoxicity, Standardization of ed. vol. ISO 10993-5, 2009, Switzerland.